



## Geohydrologic units of Ischia Island (Southern Tyrrhenian Sea, Italy)

Silvia Fabbrocino, Eliana Bellucci Sessa, Sandro de Vita, Rosario Avino, Antonio Carandente, Enrica Marotta, Fabio Todisco & Mauro Antonio Di Vito

To cite this article: Silvia Fabbrocino, Eliana Bellucci Sessa, Sandro de Vita, Rosario Avino, Antonio Carandente, Enrica Marotta, Fabio Todisco & Mauro Antonio Di Vito (2024) Geohydrologic units of Ischia Island (Southern Tyrrhenian Sea, Italy), Journal of Maps, 20:1, 2317142, DOI: [10.1080/17445647.2024.2317142](https://doi.org/10.1080/17445647.2024.2317142)

To link to this article: <https://doi.org/10.1080/17445647.2024.2317142>



© 2024 The Author(s). Published by Informa UK Limited, trading as Taylor & Francis Group on behalf of Journal of Maps.



[View supplementary material](#)



Published online: 11 Mar 2024.



[Submit your article to this journal](#)



[View related articles](#)



[View Crossmark data](#)



## Geohydrologic units of Ischia Island (Southern Tyrrhenian Sea, Italy)

Silvia Fabbrocino<sup>a,b</sup>, Eliana Bellucci Sessa<sup>b</sup>, Sandro de Vita<sup>b</sup>, Rosario Avino<sup>b</sup>, Antonio Carandente<sup>b</sup>, Enrica Marotta<sup>b</sup>, Fabio Todisco<sup>c</sup> and Mauro Antonio Di Vito<sup>b</sup>

<sup>a</sup>Department of Earth, Environment and Resources Science (DiSTAR), University of Naples Federico II, Naples, Italy; <sup>b</sup>Istituto Nazionale di Geofisica e Vulcanologia (INGV), Sezione di Napoli Osservatorio Vesuviano, Naples, Italy; <sup>c</sup>Freelance Geologist, Naples, Italy

### ABSTRACT

The first hydrogeological mapping of Ischia Island at the 1:10,000 scale is presented and discussed. The 'Map of the geohydrologic units of Ischia Island' and the accompanying hydrostratigraphic sequence at a basin scale are based on the most recent geological maps and data from the CAR.G Project, and on new volcanological and hydrogeological surveys and studies. Data sources include the database stored by the INGV, Sezione di Napoli, Osservatorio Vesuviano and field investigations, including a survey of the springs and thermo-mineral springs which has been neglected up to now. In total 130 volcanostratigraphic units and 18 geohydrologic units were recognized; the distribution of fumaroles sites was enhanced, and 60 springs/thermal springs were identified/rediscovered. The proposed hydrogeological map provides an overview of the volcano-tectonic evolution of Ischia Island and upgrades the hydrogeological model, becoming a catalyst for the effort to acquire better data and to manage natural both resources and risks.

### ARTICLE HISTORY

Received 22 November 2023  
Revised 31 January 2024  
Accepted 5 February 2024

### KEYWORDS

Hydrogeological map;  
hydrologic unit; permeability  
index; volcanic aquifer;  
thermal spring; Ischia Island

## 1. Introduction

Small volcanic islands present particular problems in assessing and managing groundwater resources, which are frequently related to intense hydrothermal circulation. This is especially true in active volcanic systems when considering the strategic role played by the exchange between groundwater systems and magmatic fluids in improving the knowledge about the possibility of phreatic explosions occurrence, and evaluating volcanic-related risks (e.g. Montanaro et al., 2022).

The geological and hydrogeological structure of such volcano active islands is crucial for the enhancement of their conceptual groundwater model, indispensable for groundwater resources protection and management.

For example, it is well known that in these terrains recent geological materials have widely varying hydraulic properties, often due to different weathering processes, as well as the function of vertical drainage or barrier of low permeability connected with dikes, depending on their geometry, age, density, fracturing. More generally, from a hydrogeological point of view, the sequence of effusive /explosive activities, associated with the major volcano-tectonic events and periods of stasis, delineates heterogeneous bodies of intercalated aquifers and aquitards, which causes in volcanic islands complex dynamic interaction among

meteoric water, sea water and fluids of deep origin (e.g. Fabbrocino et al., 2022; Herrera & Custodio, 2008; Izquierdo, 2014; Vittecoq et al., 2015).

A suitable scale map of identifiable *hydrofacies* and/or *geohydrological units* to highlight the major stratigraphic and tectonic structures of volcanic islands, which control groundwater flow, continues to be a challenge in many countries (e.g. Falkland, 1991; Madonia et al., 2021; Shahin, 2003) and needs many efforts to combine multidisciplinary information, often incomplete and fragmented in time and space.

This is a key issue even for the dynamically very active Ischia Island (Southern Tyrrhenian sea, Italy), characterized by intense hydrothermal activity, documented since the early sixteenth century by the study of Iasolino (1588), which represents the first cartography and systematic analysis of the island's thermal springs with a therapeutic aim. Despite the number of geological maps at the 1:10,000 scale (Rittmann, 1930; Sbrana et al., 2018; Sbrana & Toccaceli, 2011; Vezzoli, 1988) which, over time, have contributed to represent and update tectonic-volcanic history of the island, there is no hydrogeological mapping on the same scale up to now. Celico et al. (1999) and Piscopo, Formica, et al. (2020) are the only sources for a simplified sketch of aquifer formations on Ischia Island.

**CONTACT** Silvia Fabbrocino ✉ [silvia.fabbrocino@unina.it](mailto:silvia.fabbrocino@unina.it) 📧 Complesso Universitario di Monte Sant'Angelo, Via Vicinale Cupa Cintia, 21 - 80126 NAPOLI, Italy

📄 Supplemental data for this article can be accessed online at <https://doi.org/10.1080/17445647.2024.2317142>.

© 2024 The Author(s). Published by Informa UK Limited, trading as Taylor & Francis Group on behalf of Journal of Maps.

This is an Open Access article distributed under the terms of the Creative Commons Attribution-NonCommercial License (<http://creativecommons.org/licenses/by-nc/4.0/>), which permits unrestricted non-commercial use, distribution, and reproduction in any medium, provided the original work is properly cited. The terms on which this article has been published allow the posting of the Accepted Manuscript in a repository by the author(s) or with their consent.

Based on the most recent geological maps and data from the CAR.G Project (National Geological CARTography) (Sbrana et al., 2018; Sbrana & Toccaceli, 2011), and on new volcanological and hydrogeological surveys and studies, a novel hydrostratigraphic framework was constructed and a map of the geohydrologic units of Ischia Island was generated on a scale of 1:10,000.

The stratigraphic sequence characterization supports a process-oriented approach for underscoring the details of the geometry and extent of aquifers and confining units and so the present state of the composite volcanic aquifer system. Since recognized lithostratigraphic units have irregular depositional, tectonic, and erosional patterns, a significant part of the study was spent on finding information. This involved the collection of a range of basic data (mainly stratigraphic-logs, core analysis and pumping test results), derived from archives of local and regional public authorities and database, stored by the Istituto Nazionale di Geofisica e Vulcanologia, Sezione di Napoli, Osservatorio Vesuviano and depicted in Fabbrocino et al., 2022. It is particularly noteworthy how the collection and review of knowledge from the literature as well as from historical documents pertaining to groundwater springs were verified in the field.

On the other hand, special attention was reserved to the choice of hydrostratigraphic sequence scale, which often affects the physical properties of the aquifers. Following Möller and Volk (2015), the proposed computational/cartographic scale (1:10,000) is an effective map scale because it recognizes the operational scale at which groundwater processes occur, the location of corresponding volcano-tectonic structures, as well as the spatial visualization of their scale-specific inaccuracies.

Therefore, the designed novel map of the geohydrologic units of Ischia Island should be used in several ways. It is as a source of data, a source of information, detecting the data in hydrogeological context, and as a reference to more detailed material. It may be considered a technical/hydrogeological map to prepare effective spatial planning strategies.

## 2. Geological and volcanological contexts

The island of Ischia is the emergent part of an active and presently quiescent volcanic field, located at the north-western end of the Gulf of Naples (Italy). It rises more than 1000 m from the Southern Tyrrhenian Sea floor and is part of the Phlegraean Volcanic District, which also includes the island of Procida and the Campi Flegrei caldera (Figure 1) (Bruno et al., 2002; Orsi et al., 1999). Ischia is the result of a complex history of alternating constructive and destructive phases, which generated volcanic rocks, landslide deposits and, subordinately, sedimentary terrigenous rocks, related to volcanic, volcano-tectonic, slope instability

phenomena and intracaldera-basin marine sedimentation (Vezzoli, 1988; Barra et al., 1992a; 1992b; Tibaldi & Vezzoli, 2004; de Vita et al., 2006; 2010; Della Seta et al., 2012; 2015; 2024; Marmoni et al., 2017; Selva et al., 2019). The geological history of the island can be described according to its volcano-tectonic evolution, referring to the main caldera collapse and resurgence episodes, which strongly influenced volcanism and the morphostructural setting of the island, also conditioning the development of a complex system of groundwater and hydrothermal fluid circulation.

Volcanism at Ischia is dominated by the ignimbritic Mt. Epomeo Green Tuff (MEGT) eruptions (60–55 ky BP) that generated a caldera depression in the central part of the island (Brown et al., 2008; 2014; Sbrana et al., 2018; Sbrana & Toccaceli, 2011; Vezzoli, 1988). The caldera, partially filled by the MEGT ignimbrites, became the site of marine sedimentation and hosted a geothermal system fed by magmatic and marine fluids (Sbrana et al., 2009). Previous volcanic activity dates back to more than 150 ky, which is the age of the oldest dated rocks that are not the lowermost exposed (Vezzoli, 1988).

The Ischia volcanic activity can be summarized as follows (Brown et al., 2008; de Vita et al., 2010; Sbrana et al., 2018; Selva et al., 2019):

### 2.1. Phase 1 pre-caldera activity (150–73 ky)

This phase of activity is characterized by the occurrence of effusive and explosive eruptions that led to the emplacement of trachytic and phonolitic lava flows and domes, and a sequence of pyroclastic deposits with intercalated paleosols, that formed a volcanic field. It is presently represented by the remnant of a volcanic edifice mainly exposed in the southern part of the island (Scarrupata di Barano Formation in Vezzoli, 1988; Ancient Ischia Synthème in Sbrana & Toccaceli, 2011), and a series of small lava domes and spatter cones, which are presently exposed at the periphery of the island (volcanics older than 73 ky; Figure 1).

### 2.2. Phase 2 caldera formation and filling (60–55 ky)

The beginning of the second phase of activity is not precisely known, although a very intense period of explosive volcanism is recorded at around 60 ky, producing the highest magnitude eruptions occurred at Ischia. The deposits of at least ten explosive eruptions, fed by phonolitic to trachytic magmas, are the product of variably energetic eruptions, which generated pyroclastic density currents, fallout deposits, block and ash flows, explosion breccias and hydromagmatic dilute and turbulent pyroclastic density currents (Brown et al., 2008; Rifugio di San Nicola Synthème in Sbrana & Toccaceli, 2011; Phase 2 in Sbrana et al., 2018).



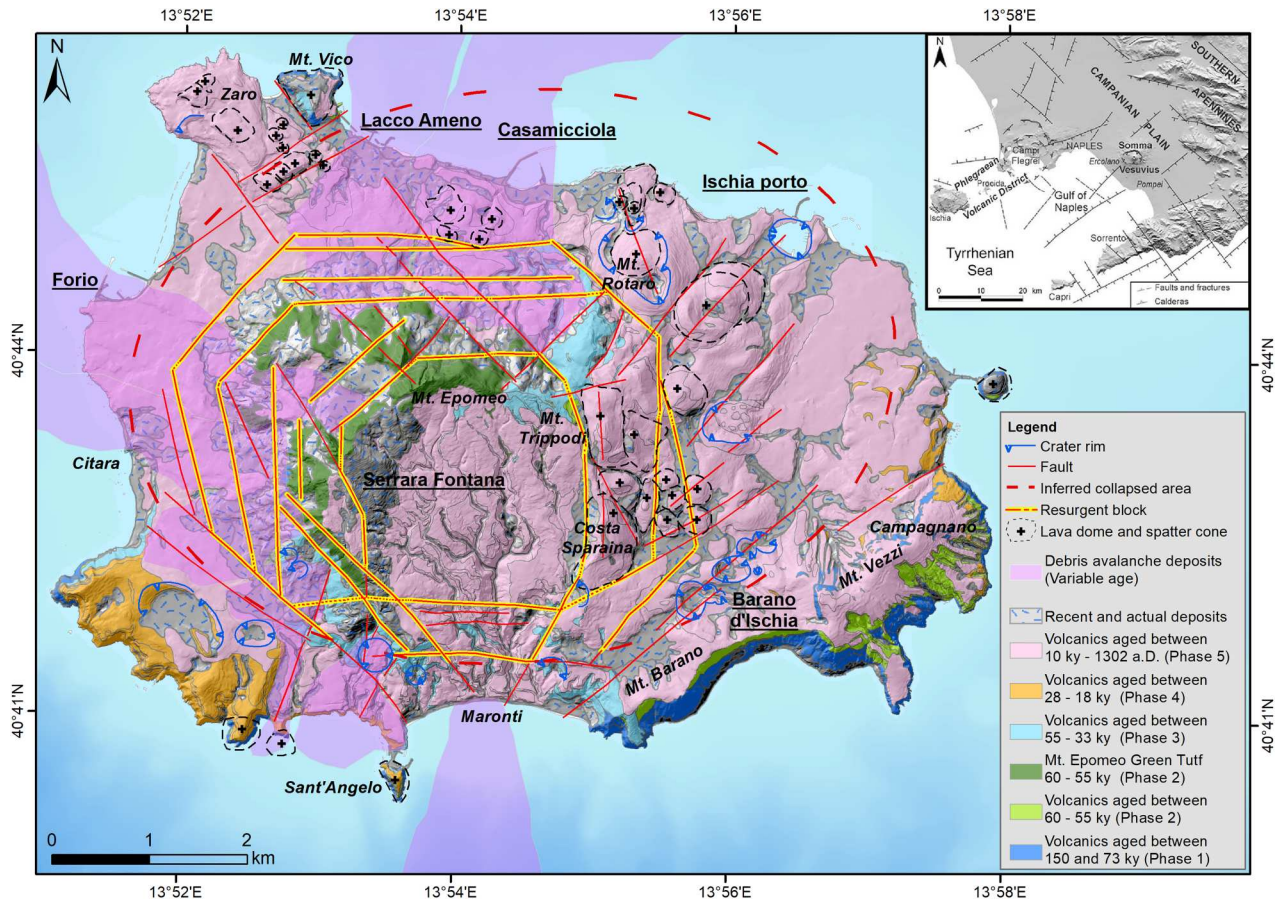


**Figure 1.** Geological and structural sketch map of Ischia Island (modified after Sbrana et al., 2018; Trasatti et al., 2019, and Della Seta et al., 2024).

This period of activity culminated with the MEGT caldera forming eruptions between 60 and 55 ky (Brown et al., 2008, and references therein; Sbrana et al., 2018; Sbrana & Toccaceli, 2011). The MEGT consists mostly of trachytic ignimbrites that partially filled the caldera depression in a submarine environment, and were also emplaced on land outside its margins.

The caldera depression was later the site of marine sedimentation, which formed a fossiliferous sequence of clays, tuffites, sandstones and siltstones by the reworking of MEGT and sedimentary supply from the mainland (Sbrana & Toccaceli, 2011).

### 2.3. Phase 3 post-caldera activity: beginning of Mt. Epomeo resurgence (55–33 ky)

The injection of new latitic and shoshonitic magmas (Brown et al., 2014; Phase 3 in Sbrana et al., 2018) induced the beginning of the asymmetric resurgence of the caldera floor, generating the Monte Epomeo block (de Vita et al., 2010; Orsi et al., 1991) and induced the emission of initially trachytic (likely residual) magmas and later latitic and mixed latitic/trachytic magmas. Volcanism of this period was characterized by a series of hydromagmatic and magmatic explosive eruptions up to 33 ky. Most of the

vents were located along the SW and NW offshore of the island, where a wide, presently submerged volcanic field was formed (Sbrana et al., 2018).

### 2.4. Phase 4 post-caldera activity: renewal of volcanism (28–18 ky)

An about 5 ky long period of quiescence predated the renewal of volcanism at 28 ky. It started with the emission of shoshonitic magmas, isotopically distinct from those characterizing the previous eruptions, suggesting the arrival of a new batch of magma into the feeding system. A new episode of caldera resurgence was likely triggered by this intrusion (Orsi et al., 1991). Differentiation of this new magma and mixing with the resident one then occurred (Casalini et al., 2017; Civetta et al., 1991; Poli et al., 1987), sporadically feeding volcanism until 18 ky (or 13 ky, Phase 4 in Sbrana et al., 2018), with the emission of shoshonitic to alkali-trachytic magmas that fed effusive and both hydromagmatic and magmatic explosive eruptions, which emplaced lava flows and Strombolian fallout deposits, and determined the construction of small tuff-cones and scoria-cones, exposed along the SE and SW coasts of the island (Campotese Subsynthème in Sbrana & Toccaceli, 2011).

### 2.5. Phase 5 post-caldera activity: renewal of caldera resurgence and volcanism (10 ky–1302 A.D.)

After another long period of quiescence, which lasted between 5 and 8 ky, a period of very sustained activity started at about 10 ky, and was fed by mainly trachytic and subordinately latitic magmas, isotopically distinct from those of the previous periods. This led [Civetta et al. \(1991\)](#) to hypothesize the arrival of a new, geochemically distinct magma into the system. Volcanism was mainly concentrated at around 5.5 ky and after 2.9 ky, with almost all the vents located in the eastern part of the island ([Figure 1](#)). Only a few vents are located outside this area, along regional fault systems or along the margins of the resurgent block. These vents generated a multi-vent lava field in the NW corner of the island, a pyroclastic sequence, exposed to the SW, and a lava dome in the N sector of the island. Since 2.9 ky, about 34 effusive and explosive, both magmatic and phreatomagmatic eruptions have taken place, generating lava domes, high-aspect ratio lava flows, tuff cones, tuff rings and variably dispersed pyroclastic-fall and current deposits, which had a very variable impact on both the island's environment and human settlements ([de Vita et al., 2010](#), and references therein; [Sbrana & Toccaceli, 2011](#); [de Vita et al., 2013](#); Phases 5 and 6 in [Sbrana et al., 2018](#)). The last eruption occurred in 1302 A.D. and generated a scoria cone and the Arso lava flow, in the NE part of the island ([de Vita et al., 2010](#)).

In the past 10 ky volcanism was characterized by the alternation of centuries of quiescence and periods of very intense activity, therefore it has been hypothesized that repeated episodes of magma intrusions occurred intermittently ([de Vita et al., 2006; 2010](#); [Tibaldi & Vezzoli, 2004](#); [Vezzoli et al., 2009](#)) likely accompanied by resurgence and periods of slope instability, with the emplacement of giant debris avalanche and landslide deposits, intercalated with volcanic deposits ([de Vita et al., 2006; 2010](#); [Della Seta et al., 2012](#)).

At present, volcanism and resurgence are quiescent, with Mt. Epomeo characterized by a moderate subsidence ([Trasatti et al., 2019](#)), suggesting that no magmatic intrusions are active at shallow depth ([Marotta et al., 2024](#)). Nevertheless the magmatic system of Ischia has to be considered still active, as testified by the intense volcanism in historical times and the very sustained geothermal fluids circulation that feeds widespread fumaroles and thermal springs ([Fabbrocino et al., 2022](#) and references therein).

### 3. Materials and methods

The map of the geohydrologic units of Ischia Island is planned to highlight the corresponding hydrogeological setting and the architecture of such a complex volcanic

aquifer system, thereby laying the basis for updating and enhancing knowledge on groundwater hydrodynamics and mineralization processes. It is part of a broader multidisciplinary research activity, and originates from an integrated view of field data and technical and scientific literature that is aimed to an operational upgrade of the hydrogeological, geochemical and volcanic monitoring system ([Fabbrocino et al., 2022](#)).

This map may be particularly useful in the conceptual phase of hydrothermal modeling and thus is supplemented with auxiliary information, such as morphology, geological, structural, hydrological, and other relevant information.

The procedure followed is in line with the preparatory synopsis of a hydrogeological map ([Struckmeier & Margat, 1995](#)) ([Figure 2](#)).

All information (geological and volcano-tectonic elements, stratigraphical logs, springs, fumaroles, well elevation, groundwater depths, groundwater levels, well discharges, geochemical data, etc) was acquired, georeferenced, verified, processed, generated, and archived in a GIS environment using the ArcGIS© ([ESRI, 2011](#)) software (rel. 10.4.1). The coordinate reference system was the WGS 84-UTM 33N.

Data sources include the database stored by the Istituto Nazionale di Geofisica e Vulcanologia, Sezione di Napoli, Osservatorio Vesuviano ([Fabbrocino et al., 2022](#)) and field investigations, among which a survey of the springs and thermo-mineral springs.

It is noteworthy that the latest geological maps of Ischia Island ([Sbrana et al., 2018](#); [Sbrana & Toccaceli, 2011](#)) – produced at scale 1:10,000 as part of the CAR.G Project (National Geological CARTography) – provide an upgrade of the geological knowledge of the examined territory, and are able to map both the shallow volcanic deposits and the morpho-structural setting, which controls the groundwater flow conditions. Therefore, the reconstruction of the hydrostratigraphic sequence ([Appendix 1](#)) and the following map of the geohydrologic units were carried out at the same cartographic scale. Furthermore, targeted geological and hydrogeological surveys were employed to revise the recognized CAR.G. lithostratigraphic units.

The geohydrologic units generated and mapped in this study are derived from the revision of the geological formation reported in CAR.G geological map, scale 1:10,000; the pattern of main volcano-tectonic elements as well as the location of springs/thermo-mineral springs and fumaroles resulted by the comparison of existing cartographic, historical, and technical/scientific documents, then verified in the field.

The topographic representation, which constitute the raster base of the map, is the topographic map created as a basis for [Vezzoli's geological map \(1988\)](#). It was georeferenced with an accuracy of 4.13 meters, and checked by the most recent orographic background derived by the Regional Technical Map ([CTR, 2004](#)),

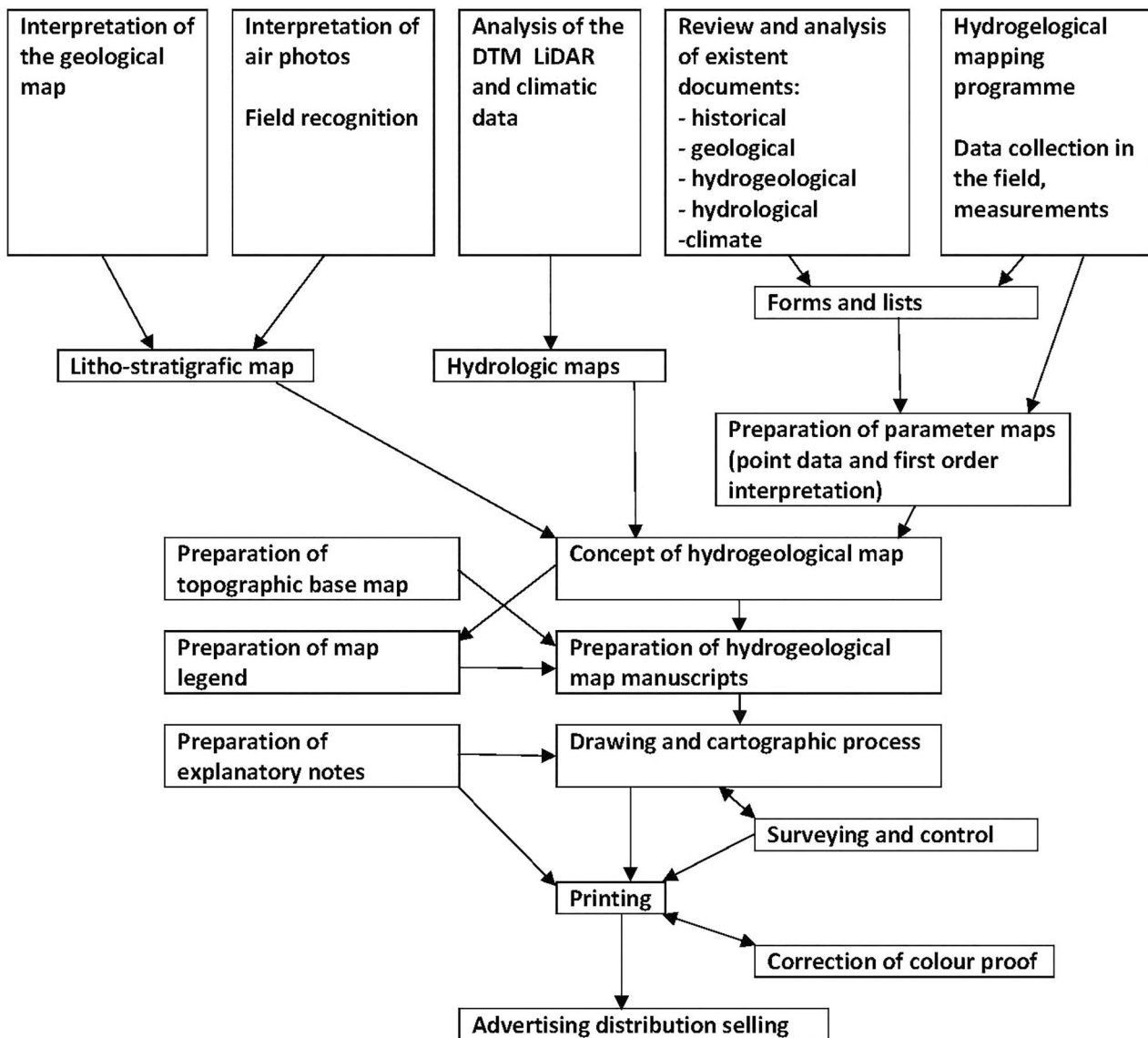


**Figure 2.** Flow chart for the preparation of the hydrogeological map (modified after Struckmeier & Margat, 1995).

scale 1:5000, and the Lidar DTM (1 x1 m ground resolution, Z error  $\pm 15$  cm, years 2009–2012).

Finally, the hydro-geo-information system generated for the proposed thematic map of Ischia Island enables the production of the following layouts: raster topographic map; polygonal and linear base map elements; polygonal, linear, and punctual attributes for geological, volcano-tectonic and hydrogeological elements as well as location of fumaroles and springs/thermo-mineral springs.

All these vector layers were graphically managed with ArcGIS© (ESRI, 2011) 10.4.1 to obtain the final map layout at the scale 1:10,000.

## 4. Results and discussion

### 4.1. Morpho-tectonic features

The volcanic system of Ischia island denotes a complex pattern of volcano-tectonic elements, partly due

to a NW-SE and NE-SW trending fault regional system. According to the scientific literature, the latter is credited with the function of transferring stress between sectors with different extensional regimes and regulate the ascent and storage of magma at lower depths (Acocella & Funicello, 2002).

The coupled analysis of main deformational features, their relationship with volcanic and non-volcanic lithostratigraphic units, and hydrogeological information reveals the effect of the main volcano-tectonic structures on fluid/groundwater flow (Fabbrocino et al., 2022 and reference therein) (Figure 3). The presence of caldera/resurgent block structures and main volcanic edifices affect the continuity of the main hydrofacies, and reveals different hydrostructure.

An important element in this regard concerns the intracalderic resurgence, characterized by a maximum uplift of the order of about 900–1100 m in the past 50 ky (Selva et al., 2019). This structure, located in the



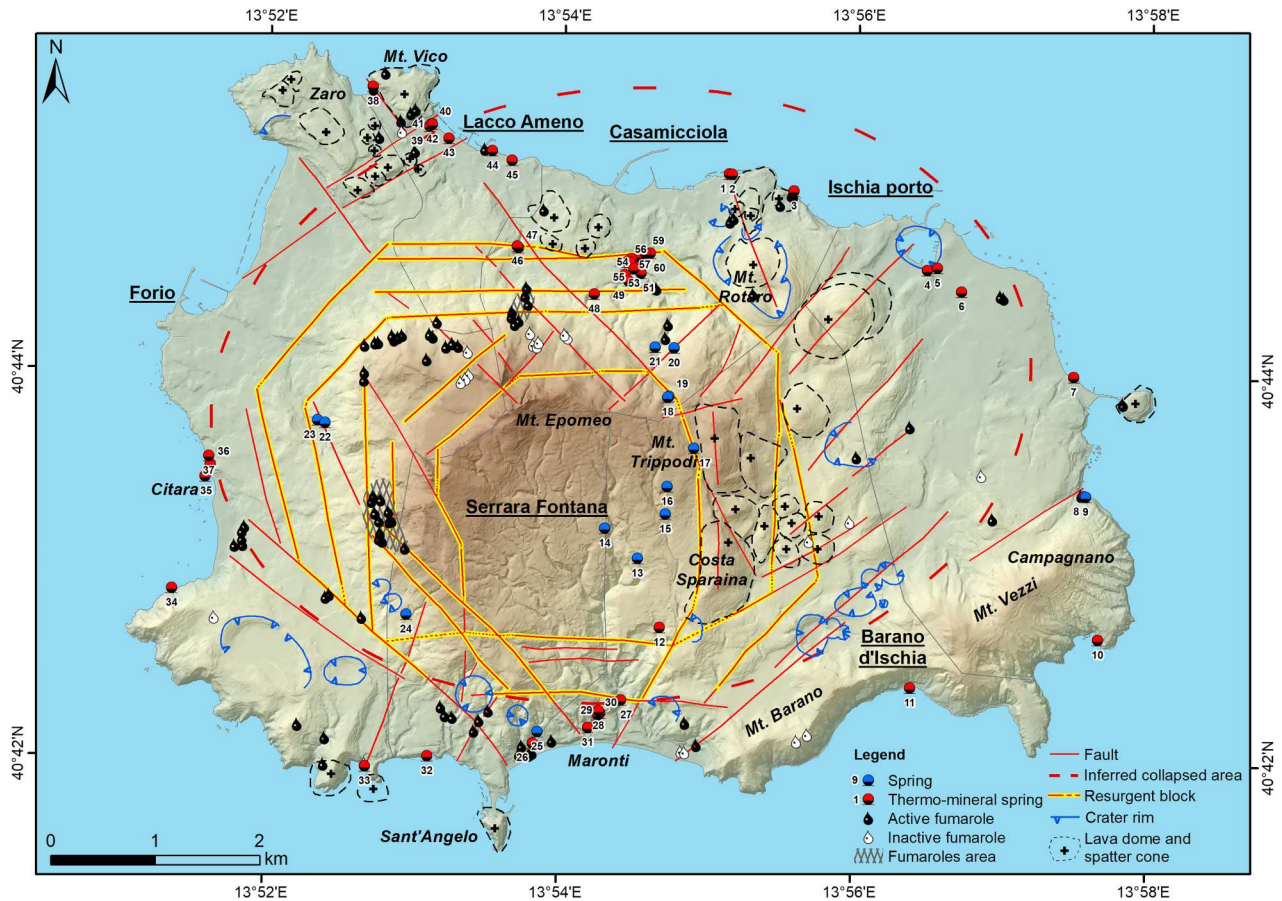


**Figure 3.** Structural sketch map of Ischia Island and layout of the springs and fumaroles. For details about the number ID of springs and thermo-mineral springs see Table 1. The Digital Elevation Model (DEM) derives from the Regional Technical Map, scale 1:5000.

central sector of the island, as a whole has a polygonal shape and see the maximum uplift in the NW portion. It is made up of differentially displaced blocks due to the reactivation of regional faults and the activation of local volcano-tectonic structures (Acocella & Funiello, 1999; Carlino et al., 2006; Marotta & de Vita, 2014; Orsi et al., 1991).

It is noteworthy that the fault systems N40-50W and N50-60E identify the sector where the resurgence processes are most active. More precisely, to the west, high-angle inward-dipping, N-S, NE-SW, and NW-SE trending faults, cut by late outward-dipping normal faults due to gravitational readjustment of the slopes, constrained the intracalderic resurgence; to the east, a number of vertical or outward-dipping N-S, NE-SW, and NW-SE trending normal faults downthrow a series of blocks, which are settled at a lower altitude and connected westward to the resurgent area (de Vita et al., 2006, 2010; Della Seta et al., 2012). Towards the N-NE coastal beach deposits are displaced at different elevation above the sea level by E-W and NW-SE trending, vertical faults (Alessio et al., 1996; Berrino et al., 2021; Carlino et al., 2022; De Novellis et al., 2018; de Vita et al., 2006; 2010; Nappi et al., 2018; 2021; Trasatti et al., 2019). As a result, the N-NE boundary of the resurgent area is not well identified.

Deformational processes are still active and characterized by subsidence, related to the cooling and deflation of a residual magma chamber (Selva et al., 2019; Sepe et al., 2007; Trasatti et al., 2019; Vezzoli et al., 2009). Thus, the resurgence process is currently passive, as revealed by geodetic data (Selva et al., 2019; Sepe et al., 2007; Trasatti et al., 2019).

Crater rims, dikes, lava domes and spatter cones, moreover, equally control the lateral and vertical variability of the lithostratigraphic units, and so of the shallower volcanic aquifer system. As shown in Figure 3, such structures are widespread in the peripheral area of the resurgent blocks, mainly to East, accordingly to the volcanological evolution of the island.

#### 4.2. Springs and fumaroles

Springs, thermal springs and fumaroles are dynamic surface features of the examined volcanic hydrothermal system, that denote complex and mutable mixing among meteoric water, sea water and deep fluids (e.g. Celico et al., 1999; Chiodini et al., 2004; Di Napoli et al., 2011; Fabbrocino et al., 2022; Piscopo, Formica, et al., 2020). Identifying their location and main characteristics is, therefore, essential to outline the aquifer properties, and to give clues about deep

hydrothermal conditions. They are so numerous and dissimilar that the most recent hydrogeological information was incomplete; in addition, ambiguous data, including location and name, have been transmitted frequently over time (Fabbrocino, 2022).

The groundwater spring inventory map (Figure 3) is the synthesis of a meticulous archival study based on the research, collection, and joint analysis of different historical sources, maps, and documents that have followed over time, and that have directly and/or indirectly involved the spring water collection systems as well as the local urban planning (see below for reference and used sources). A specific geological and hydrogeological field survey and census of existing water points (springs and wells) refines this.

In this regard, the study of Iasolino (1588) includes a map of the island, characterized by a constant cartographic scale and full of chorographic details and toponyms; it could be considered the first spring inventory map of Ischia Island. From this cartographic representation and onwards (e.g. Iovene, 1934; Italia. Ministero dei lavori pubblici. Consiglio superiore. Servizio idrografico, 1942; Rittmann, 1930; Rittman & Gottini, 1980; Santi, 1955; Sbrana et al., 2018; Sbrana & Toccaceli, 2011; Vezzoli, 1988; inventory database/maps of local and regional public authorities), continuing to analyze the technical, scientific, and historical literature concerning the springs/thermal springs and fumaroles of the island (e.g. De Siano, 1800; Chevalley De Rivaz, 1837; Marone, 1847; D'Ascia, 1867; Morgera, 1890; Grablovitz, 1893; Rebuffat, 1900; Mirabella, 1913; Ruffolo, 1923; Buchner, 1959; Celico et al., 1999; Di Napoli et al., 2011; Carlino et al., 2014; Piscopo, Formica, et al., 2020; Fabbrocino et al., 2022) a census of fumaroles and springs was carried out.

A total of 60 spring/thermal spring locations were identified/rediscovered (Figure 3); their main features are summarized in Table 1. Groundwater discharges from the volcanic aquifer system occur at an altitude that goes from 0 to about 451 m asl and the flow rate is generally a few liters per second.

The total spring flow (clearly outdated) appears to be about 10% of the estimated aquifer recharge (about 340–380 l/s; Piscopo, Formica, et al., 2020); at a basin scale, coastal groundwater discharge accounts the main natural overflow.

The areal distribution of springs and fumaroles (elevation between 0 and 557 m asl) highlights that they are commonly associated with main morpho-structural elements. They take place largely (about 93%) along the coastline and/or the caldera boundaries as well as along the main faults around the resurgent block, becoming fingerprints of the basin-scale hydrogeological processes (Figure 3); they reveal the geological/volcanological features that create transmissive pathways or barriers to flow. Thus, the main faults of the resurgent block and the caldera

boundaries should be related to barriers to horizontal groundwater flow, even if they act as vertical conduits for deep groundwater flow. In addition, the vertical displacement and the pattern of identified vents often constraint the juxtaposition of lithostratigraphic units with contrasting permeabilities.

As recognized in many hydrothermal sites (e.g. Keegan-Treloar et al., 2022 and references therein), the fault-controlled spring systems of Ischia Island, involve few contact springs (e.g. Candiano springs) and many overflow and uplift springs (Soulis, 2010), which contribute to delineate the faulted multi-aquifer setting.

### 4.3. Geohydrologic units

The map of the geohydrologic units (aquifer and confining units) of Ischia Island presents a hydrogeologic framework based on a detailed geological/volcano-tectonic approach to understanding the physical/ hydraulic characters, the geometry, and depositional setting of volcanic and nonvolcanic lithostratigraphic units. The island's volcanic activity has had both effusive and explosive eruptions and has been greatly influenced by the caldera resurgence processes since 55 ky. From a hydrogeological point of view, such complex evolution accentuates the importance of the volcanostratigraphical model; differences in the chronostratigraphic interpretation of the field outcrops, mainly related to the most recent period of volcanism (from 10ky; de Vita et al., 2010), and supported by specific field surveys and analyses of borehole data (Fabbrocino et al., 2022), made the proposed reconstruction of the hydrostratigraphic sequence at basin scale (Appendix 1) to be based on a revised model implemented on a scale of 1:10,000 by the CAR.G Project (National Geological CARTography) (Sbrana et al., 2018; Sbrana & Toccaceli, 2011). In total 130 volcanostratigraphic units were identified and labeled in Appendix 1 following the five phases of Ischia volcanic activity.

The hydrologic properties of the recognized lithostratigraphic units define and map the geohydrologic unit based on relative permeability. The properties examined are those that do not change significantly over time: permeability, porosity, transmissivity, and storage coefficient. This characterization has been extensive and complex for various motives, particularly because of the complexity of the aquifer/confining bed (often heterogenous and fractured), the quality and quantity of available data from hydrologic testing (e.g. Celico et al., 1999; Fabbrocino et al., 2022; Piscopo, Lotti, et al., 2020), and scaling issues. Although the direct evaluation (aquifer tests, laboratory permeability tests on core samples, etc.) were limited in number and quality, considerable efforts were devoted to gather, collect and integrate such



**Table 1.** Main features of springs. For details on the location of springs/thermo mineral springs see Figure 3 and the main map.

Number ID	Name	Classification	Elevation (m a.s.l.)	Temperature (°C)	Discharge (l/s)
1	Casa Coma	Thermo-mineral spring	0.13	from 17 to 56 (1936–1939); from 18 to 70 (1952–1954) (Santi, 1955)	
2	Sorgente della Scrofa	Thermo-mineral spring	0.00	from 17 to 56 (1936–1939); from 18 to 70 (1952–1954) (Santi, 1955)	
3	Sorgente di Castiglione	Thermo-mineral spring	0.00	37.5–40 (Chevalley De Rivaz, 1837; Morgera, 1890); 30–40 (Piscopo, Formica, et al., 2020)	<1 (Piscopo, Formica, et al., 2020)
4	Fornello and Fontana Springs	Thermo-mineral spring	4.09	55 (Morgera, 1890); 52 Fornello and 54 Fontana (Rebuffat, 1900); 55–58 (Iovene, 1934); 46–63 (Santi, 1955), 54–62 (Buchner, 1959); 50–60° (Rittman & Gottini, 1980)	0.86 Fontana and 1.48 Fornello (Morgera, 1890; Iovene, 1934); 2.31 (Rittman & Gottini, 1980)
5	Stabilimento Militare	Thermo-mineral spring	2.59	from 58 to 63 (Santi, 1955)	
6	Felix	Thermo-mineral spring	1.48	38 (Piscopo, Formica, et al., 2020)	2 (Piscopo, Formica, et al., 2020)
7	Bagno del Sasso	Thermo-mineral spring	0.00	36 (Santi, 1955)	
8	Carta Romana	Thermo-mineral spring	0.00	42 (Iovene, 1934); 32 (Piscopo, Formica, et al., 2020); 35.5 (July 15, 2020)	<1 (Piscopo, Formica, et al., 2020)
9	Campagnano	Spring	0.16		
10	Cefaglioli	Thermo-mineral spring	0.00		
11	Succellario	Thermo-mineral spring	0.00	50 (Iovene, 1934)	
12	Nitrodi	Thermo-mineral spring	205.23	27 (Ruffolo, 1923); 29 (Iovene, 1934); 28.1 (December, 2021)	3 (Ruffolo, 1923); 3.33 (G. Di Meglio, personal communication, December 1921)
13	Candiano Springs	Spring	322.55	8 (Iovene, 1934)	
14	Candiano Springs	Spring	396.26	8 (Iovene, 1934)	
15	Candiano Springs	Spring	350.88	8 (Iovene, 1934)	0.7 (Ruffolo, 1923 for Cava Candiano Spring)
16	Candiano Springs	Spring	418.56	8 (Iovene, 1934)	0.7 (Ruffolo, 1923 for Cava Candiano Spring)
17	Buceto Springs	Spring	451.28	8 (Iovene, 1934); 17 (July 2020)	0.92 (Ruffolo, 1923 for Buceto area)
18	Buceto Springs	Spring	414.43	8 (Iovene, 1934); 17 (July 2020)	0.92 (Ruffolo, 1923 for Buceto area)
19	Buceto Springs	Spring	408.68	8 (Iovene, 1934); 17 (July 2020)	0.92 (Ruffolo, 1923 for Buceto area)
20	Ervaniello	Spring	229.46	8 (Iovene, 1934)	
21	Acqua Piccola	Spring	226.90		
22	Pisciarello	Spring	15.52	32.5 (D'Ascia, 1867)	
22	Piellero Springs	Spring	126.52	15 (Iovene, 1934); 14 (Santi, 1955); 21 (Piscopo, Formica, et al., 2020); 21.4 (June 2020)	1.36 (Ruffolo, 1923 for Piellero Springs); < 1 (Piscopo, Formica, et al., 2020 for Piellero)
23	Piellero Springs	Spring	102.07	15 (Iovene, 1934); 15 (Santi, 1955); 21 (Piscopo, Formica, et al., 2020); 21.4 giugno 2020	1.36 (Ruffolo, 1923 for Piellero Springs); < 1 (Piscopo, Formica, et al., 2020 for Piellero)
24	Ciglio	Spring	252.28	15 (Iovene, 1934); 18 (Piscopo, Formica, et al., 2020); 18.3 (July 2020)	<1 (Piscopo, Formica, et al., 2020)
25	Cava Petrella	Spring	41.35	15 (Iovene, 1934) (Rittman & Gottini, 1980)	
26	Cava Petrella	Thermo-mineral spring	24.42		
27	Olimitello	Thermo-mineral spring	15.00	44 (Chevalley De Rivaz, 1837; Morgera, 1890); 36.5 (May 1926) (Iovene, 1934); 65–70 (1926–1930); 30 (Decembre 1952–March 1953); 28 (March 1954) in Santi, 1955, p. 26.7 (February 1969) (Mancioli, 1984); 26 (Piscopo, Formica, et al., 2020); 15 (December 2021)	1 (Piscopo, Formica, et al., 2020)
28	Cava Scura Springs	Thermo-mineral spring	25.00	70 (1926–1930); 74 (December 1952–March 1953); 68 and 82–73 (February–April 1954) in Santi, 1955, pp. 56–74 (Piscopo, Formica, et al., 2020)	2 (Piscopo, Formica, et al., 2020)
29	Cava Scura Springs	Thermo-mineral spring	23.93	41 (Decembre 2021)	
30	Cava Scura Springs	Thermo-mineral spring	20.00	74 (Iovene, 1934); 63 (December 2021)	
31	Cava Scura Springs	Thermo-mineral spring	10.00	85 (Iovene, 1934)	
32	Lo Grado	Thermo-mineral spring	0.00	75 (Iovene, 1934); 60 (July 2020)	
33	Sorgeto	Thermo-mineral spring	0.00	75 (Iovene, 1934); 82 (Piscopo, Formica, et al., 2020)	<1 (Piscopo, Formica, et al., 2020)
34	Bagno dell'Agnone di Citara	Thermo-mineral spring	0.00		
35	Citara	Thermo-mineral spring	0.00	50 (De Siano, 1800); 45.25–52.5 (D'Ascia, 1867; Marone, 1847); 45–54 (Morgera, 1890); 50–77 (wells in Iovene, 1934)	1.38 (Morgera, 1890)

(Continued)

**Table 1.** Continued.

Number ID	Name	Classification	Elevation (m a.s.l.)	Temperature (°C)	Discharge (l/s)
36	Cava dell'Isola Springs	Thermo-mineral spring	5.00	28.1 (July 2019)	
37	Cava dell'Isola Springs	Thermo-mineral spring	15.00	28.1 (July 2019)	1.5 (July 2019)
38	San Montano	Thermo-mineral spring	0.89	55 (D'Ascia, 1867; Marone, 1847); 52 (Morgera, 1890); 66 (Iovene, 1934); 40–45 (Piscopo, Formica, et al., 2020)	1.5 (Iovene, 1934); < 1 (Piscopo, Formica, et al., 2020)
39	Regina Isabella	Thermo-mineral spring	0.00	31.25–43.75 (Chevalley De Rivaz, 1837; D'Ascia, 1867); 54 (Santi, 1955); 50–70 (Rittman & Gottini, 1980 for Lacco Ameno springs); 34–55 (Piscopo, Formica, et al., 2020 for Santa Restituta group of springs)	0.86 (Morgera, 1890; Rittman & Gottini, 1980 for Lacco Ameno springs); < 1 (Piscopo, Formica, et al., 2020 for Santa Restituta group of springs)
40	Santa Restituta	Thermo-mineral spring	0.00	50 (D'Ascia, 1867; Marone, 1847); 46 (Santi, 1955)	
41	Romana	Thermo-mineral spring	0.00	31.25–43.75 (Chevalley De Rivaz, 1837; D'Ascia, 1867); 50–70 (Rittman & Gottini, 1980 for Lacco Ameno springs); 34–55 (Piscopo, Formica, et al., 2020 for Santa Restituta group of springs)	0.33 (Iovene, 1934)
42	Greca	Thermo-mineral spring	0.00	62 (Iovene, 1934); 43 (Santi, 1955)	0.26 (Iovene, 1934)
43	Bagno dell'Arena	Thermo-mineral spring	0.00	31.25–43.75 (Chevalley De Rivaz, 1837)	
44	Capitello	Thermo-mineral spring	0.00	77.5 (Chevalley De Rivaz, 1837); 80 (1931) and 56 (March 1954) in Santi, 1955, 66.25 (Morgera, 1890); 36.8 (September 2020)	
45	Mezzavia	Thermo-mineral spring			
46	La Rita Springs	Thermo-mineral spring	57.46	65–70 (Morgera, 1890); 70 (D'Ascia, 1867); from 37.5 to 40 (Morgera, 1890); 65–70 (1926–1930); 55–72 (1936–1939); 48–69 (March 1954) in Santi, 1955, 51–62 (Piscopo, Formica, et al., 2020); 42 (November 2019)	1.45 (Morgera, 1890; Rittman & Gottini, 1980)
47	La Rita Springs	Thermo-mineral spring	56.95		
48	Cava Fontana	Thermo-mineral spring	116.51	39 (Iovene, 1934); 28.6 (September 2020)	0.08 (Ruffolo, 1923); 0.06 (September 2020)
49	Sciatica	Thermo-mineral spring	76.10	62.5 (Chevalley De Rivaz, 1837); 57 (Morgera, 1890); 75 (Mirabella, 1913); 46.4 (September 2020)	
50	Sinigallia	Thermo-mineral spring	55.45	63 (Iovene, 1934); 33.9–40.7 settembre 2020	
51	Argento	Thermo-mineral spring	45.22	25–37 (Mirabella, 1913); 30.5 (September 2020)	
52	Oro	Thermo-mineral spring	51.72	40 (Mirabella, 1913)	
53	Tamburo	Thermo-mineral spring	58.55	68.75–98.75 (Chevalley De Rivaz, 1837); 98 (Marone, 1847); 98–100 (Mirabella, 1913)	
54	Ferro	Thermo-mineral spring	38.20	35 (Mirabella, 1913)	
55	Cocivola	Thermo-mineral spring	37.57	75–90 (Chevalley De Rivaz, 1837); 50–70 (Mirabella, 1913); 57–62 (Iovene, 1934)	
56	Colata	Thermo-mineral spring	39.44	81.24 (Chevalley De Rivaz, 1837); 35 (Mirabella, 1913)	
57	Occhio	Thermo-mineral spring	36.66	37.5–38.7 (Chevalley De Rivaz, 1837; D'Ascia, 1867); 38.75 (Marone, 1847); 37.5–38.5 (Grablovitz, 1893); 39 (Mirabella, 1913); 37 (Iovene, 1934)	
58	Gurgitello_Manzi	Thermo-mineral spring	39.91	64,3 (Paone, 1882); 60–65 (Morgera, 1890); 85 (Grablovitz, 1893); 55 (Iovene, 1934) and 61 (Grotte Cuotto; Iovene, 1934)	0.025 (Grablovitz, 1893)
59	Gurgitello_Belliazzi	Thermo-mineral spring	33.72	35 (Cappone, Chevalley De Rivaz, 1837; D'Ascia, 1867); from 22 to 60 (Morgera, 1890); 35 (Cappone; Grablovitz, 1893); from 56 to 64.6 (Gurgitello; Grablovitz, 1893); 53 for Gurgitello and 26 for Cappone (Iovene, 1934)	8.05 for Gurgitello and 5.13 for Sinigallia e Cotto (Morgera, 1890); 13.3 for Gurgitello, Cotto, and Sinigallia (Rittman & Gottini, 1980); 1.15 for Gurgitello springs (Iovene, 1934); 15 for Piazza Bagni groups of springs (Piscopo, Formica, et al., 2020)
60	Gurgitello_Pio Monte della Misericordia	Thermo-mineral spring	30.66	62.5–70 (Gurgitello; Chevalley De Rivaz, 1837; D'Ascia, 1867; De Siano, 1800); 60 (Morgera, 1890); 52 (Iovene, 1934)	

**Table 2.** Brief summary of the recognized geohydrologic units on Ischia Island related to the phases of volcanic activity and permeability indices.

Geohydrologic units					
Sedimentary Quaternary Deposits	Beach deposits (Permeability class: high; Flow mechanism: intergranular) (12)	Alluvial and eluvial-colluvial deposits (Permeability class: medium/high; Flow mechanism: intergranular) (13)	Slope deposits (Permeability class: medium/high; Flow mechanism: intergranular) (15)	Ancient and recent landslide deposits (Permeability class: medium/high; Flow mechanism: intergranular) (17)	Deposits of mixed origin (Permeability class: high; Flow mechanism: intergranular) (9)
	Lavas and welded scoriae (Permeability class: high; Flow mechanism: mixed) (1)	Alluvial and eluvial-colluvial deposits (Permeability class: low; Flow mechanism: intergranular) (14)	Slope deposits (Permeability class: low; Flow mechanism: intergranular) (16)	Ancient and recent landslide deposits (Permeability class: low; Flow mechanism: intergranular) (18)	Deposits of mixed origin (Permeability class: medium; Flow mechanism: intergranular) (10)
Phase 5 – post Caldera activity: renewal of Caldera resurgence and volcanism (10KY–1302 A.D.)	Lavas and welded scoriae (Permeability class: high; Flow mechanism: mixed) (1)	Beach deposits (Permeability class: high; Flow mechanism: intergranular) (12)	Pyroclastics, epiclastic and loose to partially lithified marine sediments (Permeability class: high; Flow mechanism: intergranular) (3)	Deposits of mixed origin (Permeability class: medium; Flow mechanism: intergranular) (10)	Coherent epiclastic deposits with variable degree of argillification (Permeability class: medium; Flow mechanism: mixed) (6)
	Lavas and welded scoriae (Permeability class: high; Flow mechanism: mixed) (1)	Beach deposits (Permeability class: high; Flow mechanism: intergranular) (12)	Pyroclastics, epiclastic and loose to partially lithified marine sediments (Permeability class: medium; Flow mechanism: intergranular) (4)	Deposits of mixed origin (Permeability class: low; Flow mechanism: intergranular) (11)	Coherent epiclastic deposits with variable degree of argillification (Permeability class: low; Flow mechanism: intergranular) (7)
Phase 4 – post Caldera activity: renewal of volcanism (28–18 KY)	Lavas and welded scoriae (Permeability class: high; Flow mechanism: mixed) (1)	Beach deposits (Permeability class: high; Flow mechanism: intergranular) (12)	Pyroclastics, epiclastic and loose to partially lithified marine sediments (Permeability class: high; Flow mechanism: intergranular) (3)	Deposits of mixed origin (Permeability class: medium; Flow mechanism: intergranular) (10)	Ash deposits (Permeability class: low; Flow mechanism: intergranular) (7)
	Fractured tuffs (Permeability class: medium; Flow mechanism: mixed) (2)	Beach deposits (Permeability class: high; Flow mechanism: intergranular) (12)	Pyroclastics, epiclastic and loose to partially lithified marine sediments (Permeability class: medium; Flow mechanism: intergranular) (4)	Deposits of mixed origin (Permeability class: medium; Flow mechanism: intergranular) (10)	Lithified tuffs (Permeability class: low; Flow mechanism: intergranular) (8)
Phase 3 – post Caldera activity: beginning of MT. EPOMEIO resurgence (55–33 KY)	Fractured tuffs (Permeability class: medium; Flow mechanism: mixed) (2)	Beach deposits (Permeability class: high; Flow mechanism: intergranular) (12)	Pyroclastics, epiclastic and loose to partially lithified marine sediments (Permeability class: high; Flow mechanism: intergranular) (3)	Deposits of mixed origin (Permeability class: medium; Flow mechanism: intergranular) (10)	Coherent epiclastic deposits with variable degree of argillification (Permeability class: low; Flow mechanism: intergranular) (8)
	Fractured tuffs (Permeability class: medium; Flow mechanism: mixed) (2)	Beach deposits (Permeability class: high; Flow mechanism: intergranular) (12)	Pyroclastics, epiclastic and loose to partially lithified marine sediments (Permeability class: medium; Flow mechanism: intergranular) (4)	Deposits of mixed origin (Permeability class: medium; Flow mechanism: intergranular) (10)	Lithified tuffs (Permeability class: low; Flow mechanism: intergranular) (8)

(Continued)



**Table 2.** Continued.

Geohydrologic units	
Phase 2 – Caldera formation and filling (60–55 KY)	<p>Lavas and welded scoriae (Permeability class: high; Flow mechanism: mixed) (1)</p> <p>Fractured tuffs (Permeability class: medium; Flow mechanism: mixed) (2)</p> <p>Pyroclastics, epiclastic and loose to partially lithified marine sediments (Permeability class: high; Flow mechanism: intergranular) (3)</p> <p>partially lithified marine sediments (Permeability class: medium; Flow mechanism: intergranular) (4)</p>
Phase 1 – pre-Caldera activity (>150–73 KY)	<p>Lavas and welded scoriae (Permeability class: high; Flow mechanism: mixed) (1)</p> <p>Fractured tuffs (Permeability class: medium; Flow mechanism: mixed) (2)</p> <p>Pyroclastics, epiclastic and loose to partially lithified marine sediments (Permeability class: high; Flow mechanism: intergranular) (3)</p> <p>partially lithified marine sediments (Permeability class: medium; Flow mechanism: intergranular) (4)</p> <p>Coherent epiclastic deposits with variable degree of argillification (Permeability class: low; Flow mechanism: mixed) (5)</p> <p>Lithified tuffs (Permeability class: low; Flow mechanism: intergranular) (8)</p>
	<p>Lithified tuffs (Permeability class: low; Flow mechanism: intergranular) (8)</p>

Note: For each phase of volcanic activity the degree of permeability decreases from bottom to top; each geohydrologic unit is marked with its identification number on the main map.

information from the physical properties (lithological, sedimentological, mineralogical, structural and textural characteristics) of each lithostratigraphic unit.

As a result, the system implemented for the hydrologic classification of the recognized lithostratigraphic units has been to collect both data and knowledge about the aquifers and/or geological formations, in order that their reprocessing and enhanced interpretation could not only estimate the magnitude and variability of the hydrologic properties, but also provide some insight into factor controlling the considered parameters.

The synthesis of this combination of information is the hydrostratigraphic sequence presented in Appendix 1, which can be viewed as an extended legend of the first ‘Map of the geohydrologic unit of Ischia Island’ at the 1:10,000 scale. According to the criteria of the British Geological Survey (e.g. Allen et al., 1997; Lewis et al., 2006), for each chronostratigraphical unit:

- the lithostratigraphical unit name and a brief lithological description give the combination with the CAR.G Project formations (National Geological CARtography) (Sbrana et al., 2018; Sbrana & Tocaceli, 2011) and /or lithostratigraphic units recognized in de Vita et al., 2010;
- the permeability index describes the predominant flow mechanism, specifically intergranular, fracture or mixed (intergranular and fracture), and the attributed permeability class.

The permeability index based upon known physical and hydrogeological characteristics of the lithostratigraphical units classifies the hydrostratigraphic units in qualitative terms, taking into account their age, degree of weathering, cementation/induration, and fracturing. It provides a qualitative indication of the degree of variability of permeability on the basin scale; so, contrasts in permeability from one hydrostratigraphic unit to another have allowed the distinction of three qualitative permeability classes: low, medium and high. Furthermore, the available aquifer test data (Celico et al., 1999; Piscopo, Lotti, et al., 2020; Istituto Nazionale di Geofisica e Vulcanologia, Sezione di Napoli, Osservatorio Vesuviano database) may suggest a likely range of hydraulic conductivity (k) for the identified permeability classes:

- high permeability,  $k > 10^{-3}$  m/s;
- medium permeability,  $10^{-4} < k < 10^{-3}$  m/s;
- low permeability,  $10^{-9} < k < 10^{-4}$  m/s.

In this way, eighteen geohydrologic units (a lithostratigraphic unit, or a group of lithostratigraphic units, that by virtue of its hydraulic properties has a dominant flow mechanism and a small range of permeability values) have been identified on Ischia Island.

Finally, they classify the lithostratigraphic units according to their capacity to transmit, store and yield water (aquifer or confining unit) and identify the basic unit of the hydrogeological map: their extension, structure, and geometry characterize the aquifer systems and affect/depict the groundwater flow. In short, the identification of these geohydrologic units reveals the impact of volcano-tectonic features on the groundwater circulation.

Table 2 outlines the detected geohydrologic units according to the phases of volcanic activity and the permeability index.

## 5. Conclusions

The ‘Map of the geohydrologic units of Ischia Island’ is the first hydrogeological mapping of the island at the 1:10,000 scale. The 18 recognized geohydrologic units, the 60 identified/rediscovered springs/thermal springs, and the distribution of fumaroles sites provide a comprehensive overview of the volcano-tectonic evolution of the island and its related groundwater flow conditions. This map therefore consists of a synthesis of knowledge about the variability and controls on the hydrological properties of the labeled lithostratigraphic units. It involves and combines information collected from new volcanological/ geochemical/ hydrogeological surveys, tests on aquifer material at varying scales, and groundwater observations, from published and unpublished literature and from historical sources/maps/ documents (the latter becoming very significant in areas where hydrogeological data, including location and name of springs, are few and ambiguous; see all the cited references).

The accompanying hydrostratigraphic sequence at basin scale (Appendix 1) and the characterization of the geohydrologic units based upon fundamental physical properties (in a hydrogeological sense), which are in general time invariant, make the map a useful tool for in-depth investigations, examination and analysis of the composite hydrothermal system of the discussed active volcanic island. The database which underpins this map (depicted in Fabbrocino et al., 2022) represents a starting point for the development of a more thorough, and thus more operational hydrogeological, geochemical and volcanic monitoring system.

The creation of this map at a suitable survey-scale and the construction of the related database has emphasized the complex architecture of the volcanic aquifer system and the variable (and often poor or outdated) quality of the hydrogeological data available, becoming a catalyst for the effort to acquire better data and to protect, restore and promote the sustainable use of the territory.

A rigorous scientific process is followed by the developed cartographic project for a basic geological/

hydrogeological map, which satisfies the current and essential socio-economic needs of territories that require managing natural both resources and hazards/risks. In such a case, a technical/hydrogeological map is essential for designing effective territorial/environmental planning and risk management strategies. Hydrogeological information generated on a scale of 1:10,000 makes it possible to give priority to the recurrence and distribution of the cover deposits, or to detail the geohydrologic unit outcrops which constitute the shallower layers of the subsoil; at the same time, it ensures that the morphostructural setting, which controls the basal aquifer and/or confining units and so the groundwater flow conditions, is not neglected.

The analysis of the resulting ‘Drainage basins and permeability map’ (shown in the main map), in terms of the distribution and size of areas with different permeability, becomes, therefore, interesting. The shallow aquifer system shows significant hydrostratigraphic and volcano-tectonic features, which confirm and enhance the previous conceptual hydrogeological model of Ischia Island.

The geohydrologic units composed of ‘Lavas and welded scoriae’ and ‘Fractured tuffs’, where the flow mechanism is mixed (intergranular and fracture), are the main aquifers; to these are added the loose to partially lithified pyroclastic and sedimentary deposits, ranging from high to medium permeability (Figure 4).

The coherent epiclastic and marine deposits (mixed flow mechanism) from the main periods of stasis and ‘Lithified tuffs’, instead, confine and constrain the groundwater flow; they, given their areal distribution, contribute to create a multi-flow system. A widely variable permeability combination occurs within the sedimentary Quaternary deposits, which cover most of this volcanic terrain; it was related to the characteristics of both processes and sediments of origin. These shallower geohydrologic units and their mutable permeability classes influence the infiltration and runoff processes as well as the location of the springs (‘cold waters’), underlying the morphostructural control even on the shallowest groundwater flow.

Moreover, it is important to consider the main aquifer framework and fault- controlled spring systems associated with the distribution of the fumaroles sites (cf. Section 4.2) on Ischia Island. The map of the geohydrologic units and related additional hydrostratigraphic sequence at 1:10,000 scale reveal, in this way, the delimitation of rather homogeneous stratigraphic and volcano-tectonic structures at the basin-scale, as has been described in the previous studies (Fabbrocino et al., 2022). In this regard, the volcano-tectonic structure of the resurgent block is certainly noteworthy, but this map portray information on relationship between caldera/resurgent block and main eruptive vents that, if we consider the potential

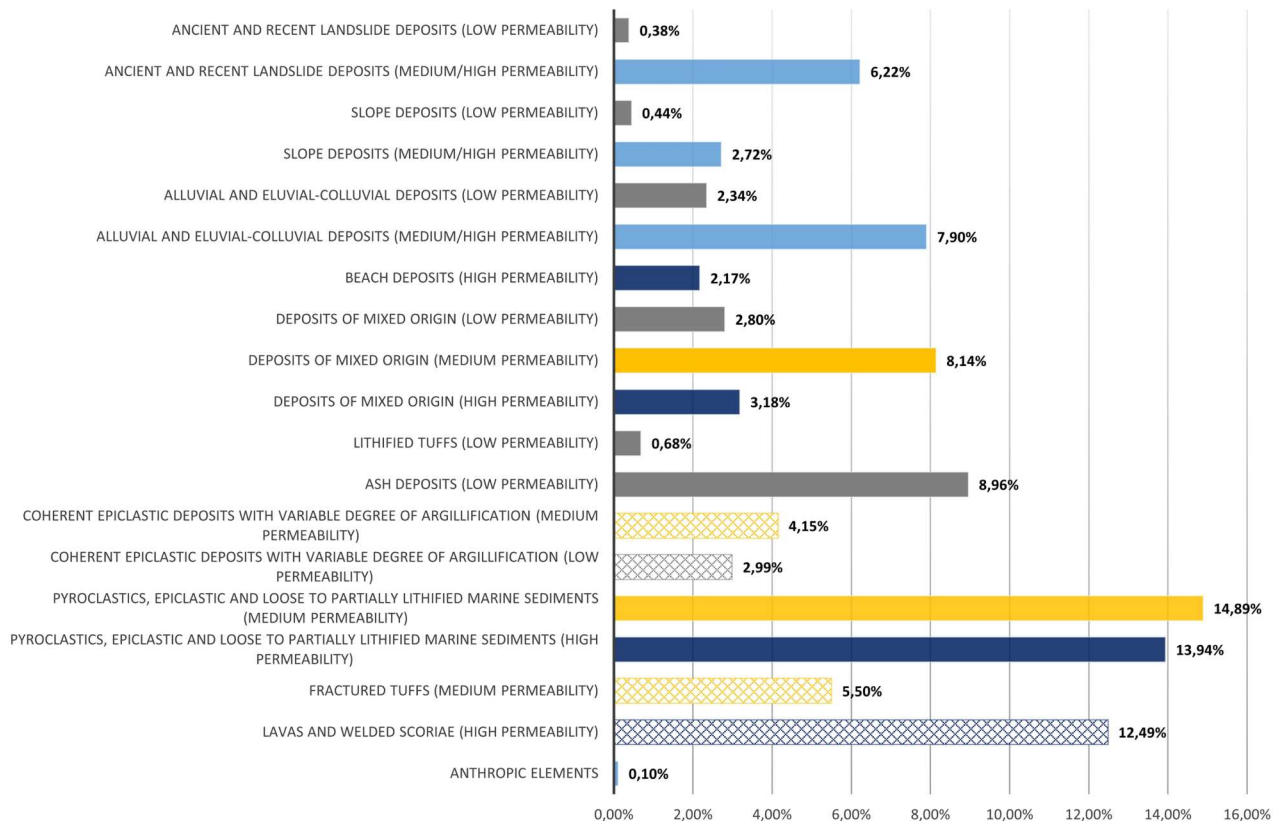


**Figure 4.** Outcrop areas and permeability classes of the identified geohydrologic units represented as a percentage of the volcanic terrain area. For each geohydrologic unit the solid color marks the intergranular flow mechanism; the pattern the mixed flow.



for the future, could contribute to improve the better characterization of several different hydrostructures. The upgrade of the general hydrogeological model, where the so-called ‘basal aquifer’ cannot be considered continuous, will implement a better volcanological, hydrogeological, and geochemical monitoring for environmental planning and protection policies.

### Software

ArcGIS 10.4.1 (ESRI) was used to georeference the topographic map, elaborate the digital elevation model from CTR, and mosaic the LIDAR data of the Città Metropolitana di Napoli. ArcGIS 10.4.1 (ESRI) was used to digitize, verify and modify the vector data used to process new geographical information based on new acquisitions. The final layout of the map was designed and created using ArcGIS 10.4.1 (ESRI).

### Acknowledgements

The study reported herein follows the preparatory studies conducted by the University of Naples Federico II as part of the Project ‘Groundwater and Energy: a strategy for the sustainable development’ (CUP: E64D17000030002; P.O.R. Campania FSE 2014-2020. – AXIS III ‘Education and training’ – Specific Objective 14 ‘Increase of skills, the workforce and facilitation of mobility, employment/ understanding’ – Action 10.4.7 ‘Internships and mobility initiatives, also transnational, as privileged opportunities for learning and professionalization’) coordinated by Silvia Fabbrocino. A particular acknowledgement goes to Antonio Giardino and Lucia Marino, whose curiosity and enthusiasm during their graduation studies under the supervision of S. Fabbrocino at the University of Naples, first shone a light on the marvelous island of Ischia. The authors express their gratitude to all the representatives of the institutions involved and particularly all islanders and hotel managers for the support provided during the investigation. The authors have also the privilege of express their gratitude to Pasquale Belviso for the operational contribute during field investigations and Prof. Antonietta Iacono for her support in analyzing historical background. This work is dedicated to the memory of don Angelo Iacono, parish priest of the Church of San Ciro al Ciglio. And finally, the authors are grateful to the reviewers Dr Jiří Pánek, Prof. Domenico Guida, and Dr Steven Bernard, and to the Editors Dr Mike Smith and Prof. Jasper Knight for their highly qualified comments that drove a detailed refinement of the map and the manuscript.

### Disclosure statement

No potential conflict of interest was reported by the author(s).

### Funding

This work was supported by INGV project Pianeta Dinamico – Working Earth (CUP 1466 D53J19000170001 – Fondo finalizzato al rilancio degli investimenti delle 1467 amministrazioni centrali dello Stato e allo sviluppo del

Paeseà, legge 145/2018) – Theme 2 TIFEHO [grant number CUP 1466 D53J19000170001].

### Author Contributions

SF, SV, and MV contributed to conceptualization, data validation, and reviewing and editing the manuscript. SF and EB performed data curation and formal analysis. SF, SV, MV, RA, AC, EM and FT carried out investigations. SF contributed to designing the methodology and wrote the first draft of the manuscript. SF, EB, and SV drew the map and figures. SV was responsible for funding acquisition and project administration. All authors contributed to manuscript revision and read and approved the submitted version.

### Data availability statement

The raw data supporting the conclusions of this article will be made available by the authors, without undue reservation.

### References

- Acocella, V., & Funiciello, R. (1999). The interaction between regional and local tectonics during resurgent doming: The case of the island of Ischia, Italy. *Journal of Volcanology and Geothermal Research*, 88(1-2), 109–123. [https://doi.org/10.1016/S0377-0273\(98\)00109-7](https://doi.org/10.1016/S0377-0273(98)00109-7)
- Acocella, V., & Funiciello, R. (2002). Transverse structures and volcanic activity along the Tyrrhenian margin of central Italy. *Bollettino Della Società Geologica Italiana*, 1(1), 739–747.
- Alessio, G., Esposito, E., Ferranti, L., Mastrolorenzo, G., & Porfido, S. (1996). Correlazione tra sismicità ed elementi strutturali nell’isola d’Ischia. *Il Quaternario*, 9(1), 303–308.
- Allen, D. J., Brewerton, L. J., Coleby, L. M., Gibbs, B. R., Lewis, M. A., MacDonald, A. M., Wagstaff, S. J., & Williams, A. T. (1997). The physical properties of major aquifers in England and Wales. *British Geological Survey Technical Report WD/97/34*, 312. Environment Agency R&D Publication
- Barra, D., Cinque, A., Italiano, A., & Scorziello, R. (1992a). Il Pleistocene superiore marino di Ischia: Paleoecologia e rapporti con l’evoluzione tettonica recente. *Studi Geologici Camerti*, 1, 231–243.
- Barra, D., Italiano, A., Allegri, L., Belluomini, G., & Manfra, L. (1992b). La serie marina olocenica di Cafieri (isola d’Ischia): Implicazioni vulcano-tettoniche e geomorfologiche. *Il Quaternario*, 5(1), 17–26.
- Berrino, G., Vajda, P., Zahorec, P., Camacho, A. G., De Novellis, V., Carlino, S., Papco, J., Bellucci Sessa, E., & Czikhardt, R. (2021). Interpretation of spatiotemporal gravity changes accompanying the earthquake of 21 August 2017 on Ischia (Italy). *Contributions to Geophysics and Geodesy*, 51(4), 345–371. <https://doi.org/10.31577/congeo.2021.51.4.3>
- Brown, R. J., Civetta, L., Arienzo, I., D’Antonio, M., Moretti, R., Orsi, G., Tomlinson, E. L., Albert, P. G., & Menzies, M. A. (2014). Geochemical and isotopic insights into the assembly, evolution and disruption of a magmatic plumbing system before and after a cataclysmic caldera-collapse eruption at Ischia volcano (Italy). *Contributions to Mineralogy and Petrology*, 168(3), 1035. <https://doi.org/10.1007/s00410-014-1035-1>

- Brown, R. J., Orsi, G., & de Vita, S. (2008). New insights into late Pleistocene explosive volcanic activity and caldera formation on Ischia (southern Italy). *Bulletin of Volcanology*, 70(5), 583–603. <https://doi.org/10.1007/s00445-007-0155-0>
- Bruno, P., de Alteriis, G., & Florio, G. (2002). The western undersea section of the Ischia volcanic complex (Italy, Tyrrhenian Sea) inferred by marine geophysical data. *Geophysical Research Letters*, 29(9), 2689–2692. <https://doi.org/10.1029/2001GL013904>
- Buchner, P. (1959). *Storia degli stabilimenti termali di Porto d'Ischia*. EDITUR.
- Carlino, S., Cubellis, E., Luongo, G., & Obrizzo, F. (2006). On the mechanics of caldera resurgence of Ischia island (southern Italy). *Geological Society, London, Special Publications*, 269(1), 181–193. <https://doi.org/10.1144/GSL.SP.2006.269.01.12>
- Carlino, S., Sbrana, A., Pino, N. A., Marianelli, P., Pasquini, G., De Martino, P., & De Novellis, V. (2022). The volcano-tectonics of the northern sector of Ischia island caldera (Southern Italy), Resurgence. *Frontiers in Earth Science*, 10. <https://doi.org/10.3389/feart.2022.730023>
- Carlino, S., Somma, R., Troiano, A., Di Giuseppe, M. G., Troise, C., & De Natale, G. (2014). The geothermal system of Ischia Island (southern Italy): Critical review and sustainability analysis of geothermal resource for electricity generation. *Renewable Energy*, 62, 177–196. <https://doi.org/10.1016/j.renene.2013.06.052>
- Carta Tecnica Regionale CTR. (2004). Geoportale Regione Campania. <https://sit2.regione.campania.it/servizio/carta-tecnica-regionale>
- Casalini, M., Avanzinelli, R., Heumann, A., de Vita, S., Sansivero, F., Conticelli, S., & Tommasini, S. (2017). Geochemical and radiogenic isotope probes of Ischia volcano, southern Italy: Constraints on magma chamber dynamics and residence time. *American Mineralogist*, 102(2), 262–274. <https://doi.org/10.2138/am-2017-5724>
- Celico, P., Stanzione, D., Esposito, L., Formica, F., Piscopo, V., & De Rosa, B. M. (1999). La complessità idrogeologica di un'area vulcanica attiva: l'Isola d'Ischia (Napoli-Campania). *Bollettino Società Geologica Italiana*, 118, 485–504.
- Chevalley De Rivaz, J. E. (1837). Description des eaux minero-thermales et des etuves de l'Île d'Ischia / par J.E. Chevalley de Rivaz. In G. Glass (Ed.), *reveu, augmentation et ornee d'une carte d'Ischia. A Naples: chez l'auteur: chez George Glass* (Vol. VIII, 3rd ed, pp. 182). George Glass.
- Chiodini, G., Avino, R., Brombach, T., Caliro, S., Cardellini, C., De Vita, S., Frondini, F., Granieri, D., Marotta, E., & Ventura, G. (2004). Fumarolic and diffuse soil degassing west of Mount Epomeo, Ischia, Italy. *Journal of Volcanology and Geothermal Research*, 133(1-4), 291–309. [https://doi.org/10.1016/S0377-0273\(03\)00403-7](https://doi.org/10.1016/S0377-0273(03)00403-7)
- Civetta, L., Gallo, G., & Orsi, G. (1991). Sr- and Nd- isotope and trace-element constraints on the chemical evolution of the magmatic system of Ischia (Italy) in the last 55 ka. *Journal of Volcanology and Geothermal Research*, 46(3-4), 213–230. [https://doi.org/10.1016/0377-0273\(91\)90084-D](https://doi.org/10.1016/0377-0273(91)90084-D)
- D'Ascia, G. (1867). *Storia dell'isola d'Ischia / descritta da Giuseppe D'Ascia*. Napoli pp. 527.
- Della Seta, M., Esposito, C., Fiorucci, M., Marmoni, G. M., Martino, S., Sottili, G., Belviso, P., Carandente, A., de Vita, S., Marotta, E., & Peluso, R. (2024). Thermal monitoring to infer possible interactions between shallow hydrothermal system and slope-scale gravitational deformation of Mt. Epomeo (Ischia Island, Italy). In E. Marotta, L. D'Auria, F. Zaniboni, & R. Nave (Eds.), *Volcanic island: From hazard assessment to risk mitigation*. *Geological society* (519, pp. 5–27). Special Publications. <https://doi.org/10.1144/SP519-2020-131>
- Della Seta, M., Esposito, C., Marmoni, G. M., Martino, S., Paciello, A., Perinelli, C., & Sottili, G. (2015). Geological constraints for a conceptual evolutionary model of the slope deformations affecting Mt. Nuovo at Ischia (Italy). *Italian Journal of Engineering Geology and Environment*, 2, 15–29. <https://doi.org/10.4408/IJEGE.2015-02.O-04>
- Della Seta, M., Marotta, E., Orsi, G., de Vita, S., Sansivero, F., & Fredi, P. (2012). Slope instability induced by volcano-tectonics as an additional source of hazard in active volcanic areas: The case of Ischia island (Italy). *Bulletin of Volcanology*, 74(1), 79–106. <https://doi.org/10.1007/s00445-011-0501-0>
- De Novellis, V., Carlino, S., Castaldo, R., Tramelli, A., De Luca, C., Pino, N. A., Pepe, S., Convertito, V., Zinno, I., De Martino, P., Bonano, M., Giudicepietro, F., Casu, F., Macedonio, G., Manunta, M., Cardaci, C., Manzo, M., Di Bucci, D., Solaro, G., ... Tizzani, P. (2018). The 21 August 2017 Ischia (Italy) earth-quake source model inferred from seismological, GPS, and DInSAR measurements. *Geophysical Research Letters*, 45(5), 2193–2202. <https://doi.org/10.1002/2017GL076336>
- De Siano, F. (1800). *Brevi, e succinte notizie di storia naturale, e civile dell'isola d'Ischia. Del dottor fisico d. Francesco De Siano per servire di guida, e comodo ai viaggiatori, ed a quei, che debbono fare uso delle acque, e fumarole di detta isola*.
- de Vita, S., Di Vito, M., Gialanella, C., & Sansivero, F. (2013). The impact of the Ischia Porto tephra eruption (Italy) on the Greek colony of Pithekoussai. *Quaternary International*, 303, 142–152. <https://doi.org/10.1016/j.quaint.2013.01.002>
- de Vita, S., Sansivero, F., Orsi, G., & Marotta, E. (2006). Cyclical slope instability and volcanism related to volcano-tectonism in resurgent calderas: The Ischia Island (Italy) case study. *Engineering Geology*, 86(2-3), 148–165. <https://doi.org/10.1016/j.enggeo.2006.02.013>
- de Vita, S., Sansivero, F., Orsi, G., Marotta, E., & Piochi, M. (2010). Volcanological and structural evolution of the Ischia resurgent caldera (Italy) over the past 10 ky. In G. Groppe & L. Vierck-Goette (Eds.), *Stratigraphy and geology of volcanic areas*, The geological society of America, special paper, 464 (pp. 193–239). The geological society of America. [https://doi.org/10.1130/2010.2464\(10\)](https://doi.org/10.1130/2010.2464(10))
- Di Napoli, R., Martorana, R., Orsi, G., Aiuppa, A., Camarda, M., Gregorio, D., Gagliano, S., Candela, E., Luzio, D., Messina, N., Pecoraino, G., Bitetto, M., de Vita, S., & Valenza, M. (2011). The structure of a hydrothermal system from an integrated geochemical, geophysical, and geological approach: The Ischia Island case study. *Geochemistry, Geophysics, Geosystems*, 12(7), 1–25. <https://doi.org/10.1029/2010GC003476>
- ESRI. (2011). *Arcgis desktop: Release 10; environmental systems research institute*. Inc.
- Fabbrocino, S. (2022). Le acque minerali e termali tra sostenibilità e sviluppo socioeconomico da Plinio il Vecchio all'Agenda 2030. In R. Valenti, C. Renda, A. Prenner, M. Paladini, & M. Cozzolino (Eds.), *SPA: SALUS PER AQUAM Saperi e tecniche del termalismo tra antico e moderno. Quaderni di «Invigilata Lucernis»* (50, pp. 107–118). Edipuglia. <https://doi.org/10.4475/0277>

- Fabbrocino, S., Bellucci Sessa, E., de Vita, S., Di Vito, A. M., Avino, R., & Marotta, E. (2022). A GIS-based hydrogeological approach to the assessment of the groundwater circulation in the Ischia volcanic island (Italy). *Frontiers in Earth Science*, 10, 883719. <https://doi.org/10.3389/feart.2022.883719>
- Falkland, A. (1991). *Hydrology and water resources of small islands: A practical guide*. UNESCO. p. 435.
- Grablovitz, G. (1893). Sulle acque termali dell'isola d'Ischia con riguardo a quelle del Gurgitello: Note rimesse per la pubblicazione negli Annali al R. Ufficio Centrale di Meteorologia e Geodinamica in Roma / Giulio Grablovitz. Casamicciola Terme: Casa Editrice "Le Maree" 1876, 2000. Ristampa dell'ediz.: Napoli, R. Stabilimento Tipografico De Angelis-Bellisario, 1893.
- Herrera, C., & Custodio, E. (2008). Conceptual hydrogeological model of volcanic Easter Island (Chile) after chemical and isotopic surveys. *Hydrogeology Journal*, 16(7), 1329–1348. <https://doi.org/10.1007/s10040-008-0316-z>
- Iasolino, G. (1588). De' rimedi naturali che sono nell'isola di Pithecusa hoggi detta Ischia. Libri due. Et in questa seconda impressione ricorretto et accresciuto con alcune annotazioni del dr. filosofo sig. Gio. Postoya. E nell'ultimo aggiunti li bagni d'Ischia di Gio. Elisio medico napoletano. Con due figure e pianta della deta isola, in Napoli.
- Iovene, F. (1934). La termicità dell'Isola d'Ischia. Tesi di laurea.
- Italia. Ministero dei lavori pubblici. Consiglio superiore. Servizio idrografico. (1942). *Le Sorgenti italiane: Elenco e descrizione*. Campania. Sezione Idrografica di Napoli. VII, pp. 746, Istituto poligrafico dello Stato.
- Izquierdo, T. (2014). Conceptual hydrogeological model and aquifer system classification of a small volcanic island (La Gomera; Canary Islands). *Catena*, 114, 119–128. <https://doi.org/10.1016/j.catena.2013.11.006>
- Keegan-Treloar, R., Irvine, D. J., Sol'orzano-Rivas, S. C., Werner, A. D., Banks, E. W., & Currell, M. J. (2022). Fault-controlled springs: A review. *Earth-Science Reviews*, 230, 104058. <https://doi.org/10.1016/j.earscirev.2022.104058>
- Lewis, M. A., Cheney, C. S., & Odochartaigh, B. E. (2006). Guide to permeability indices. *British Geological Survey Open Report, CR/06/160N*, 29.
- Madonia, P., Campilongo, G., Cangemi, M., Carapezza, M. L., Inguaggiato, S., Ranaldi, M., & Vita, F. (2021). Hydrogeological and geochemical characteristics of the Coastal Aquifer of Stromboli Volcanic Island (Italy). *Water*, 13(4), 417. <https://doi.org/10.3390/w13040417>
- Mancioli, M. (1984). Le proprietà terapeutiche delle acque Nitrodi e Olmitello. *Barano- Isola D'Ischia. Li Causi editore*, 109.
- Marmoni, G., Martino, S., Heap, M. J., & Reuschlé, T. (2017). Gravitational slope deformation of a resurgent caldera: New insights from the mechanical behaviour of Mt. Nuovo tuffs (Ischia Island, Italy). *Journal of Volcanology and Geothermal Research*, 345, 1–20. <https://doi.org/10.1016/j.jvolgeores.2017.07.019>
- Marone, V. (1847). *Memoria contenente un breve ragguaglio dell'isola d'Ischia e delle acque minerali arene termali e stufe vaporose, che vi scaturiscono colle loro proprieta fisiche chimiche e medicinali da servire di norma a coloro che ne debbono far uso*. Tipografia Gennaro Agrelli.
- Marotta, E., Berrino, G., de Vita, S., Di Vito, M., & Camacho, A. G. (2024). Structural setting of the Ischia resurgent caldera (Southern Tyrrhenian Sea, Italy) by integrated 3D gravity inversion and geological models. In E. Marotta, L. D'Auria, F. Zaniboni, & R. Nave (Eds.), *Volcanic island: From hazard assessment to risk mitigation*. Geological society (519, pp. 29–546). Special Publications. <https://doi.org/10.1144/SP519-2022-129>
- Marotta, E., & de Vita, S. (2014). The role of pre-existing tectonic structures and magma chamber shape on the geometry of resurgent blocks: Analogue models. *Journal of Volcanology and Geothermal Research*, 272, 23–38. <https://doi.org/10.1016/j.jvolgeores.2013.12.005>
- Mirabella, V. (1913). *Cenni storici e Guida dell'isola d'Ischia*. Napoli Tipografia Francesco Tramontano.
- Möller, M., & Volk, M. (2015). Effective map scales for soil transport processes and related process domains — Statistical and spatial characterization of their scale-specific inaccuracies. *Geoderma*, 247–248, 151–160. <https://doi.org/10.1016/j.geoderma.2015.02.003>
- Montanaro, C., Mick, E., Salas-Navarro, J., Caudron, C., Cronin, S. J., Maarten de Moor, J., Scheu, B., Stix, J., & Strehlow, K. (2022). Phreatic and hydrothermal eruptions: From overlooked to looking over. *Bulletin of Volcanology*, 84(6), 1–16. <https://doi.org/10.1007/s00445-022-01571-7>
- Morgera, V. (1890). *Le Terme dell'isola d'Ischia prima e dopo gli ultimi terremoti distruttivi, 4 marzo 1881 e 28 luglio 1883: studi ed osservazioni*. Lanciano e D'Ordia.
- Nappi, R., Alessio, G., Gaudiosi, G., Nave, R., Marotta, E., Siniscalchi, V., Civico, R., Pizzimenti, L., Peluso, R., Belviso, P., & Porfido, S. (2018). The 21 august 2017 md 4.0 Casamicciola earthquake: first evidence of Coseismic Normal surface faulting at the Ischia Volcanic Island. *Seismological Research Letters*, 89(4), 1323–1334. <https://doi.org/10.1785/0220180063>
- Nappi, R., Porfido, S., Paganini, E., Vezzoli, L., Ferrario, M. F., Gaudiosi, G., Alessio, G., & Michetti, A. M. (2021). The 2017, MD = 4.0, Casamicciola earthquake: ESI-07 scale evaluation and implications for the source model. *Geosciences*, 11(2), 44. <https://doi.org/10.3390/geosciences11020044>
- Orsi, G., Gallo, G., & Zanchi, A. (1991). Simple-shearing block resurgence in caldera depression. A model from Pantelleria and Ischia. *Journal of Volcanology and Geothermal Research*, 47(1-2), 1–11. [https://doi.org/10.1016/0377-0273\(91\)90097-J](https://doi.org/10.1016/0377-0273(91)90097-J)
- Orsi, G., Patella, D., Piochi, M., & Tramacere, A. (1999). Magnetic modelling of the Phlegrean volcanic district with extension to the Ponza archipelago, Italy. *Journal of Volcanology and Geothermal Research*, 91(2-4), 345–360. [https://doi.org/10.1016/S0377-0273\(99\)00043-8](https://doi.org/10.1016/S0377-0273(99)00043-8)
- Paone, D. B. (1882). *Isola d'Ischia Stazione climatica-balnearia. Utili ricordi*. Vincenzo Bona.
- Piscopo, V., Formica, F., Lana, L., Lotti, F., Pianese, L., & Trifuoggi, M. (2020). Relationship between aquifer pumping response and quality of water extracted from wells in an active hydrothermal system: The case of the Island of Ischia (southern Italy). *Water*, 12(9), 2576. <https://doi.org/10.3390/w12092576>
- Piscopo, V., Lotti, F., Formica, F., Lana, L., & Pianese, L. (2020). Groundwater flow in the Ischia volcanic island (Italy) and its implications for thermal water abstraction. *Hydrogeology Journal*, 28(2), 579–601. <https://doi.org/10.1007/s10040-019-02070-4>
- Poli, S., Chiesa, S., Gillot, P. Y., Gregnanin, A., & Guichard, F. (1987). Chemistry versus time in the volcanic complex of Ischia (Gulf of Naples, Italy): Evidence of successive magmatic cycles. *Contributions to Mineralogy and Petrology*, 95(3), 322–335. <https://doi.org/10.1007/BF00371846>
- Rebuffat, O. (1900). *Acque delle Terme di Fornello e Fontana in Porto d'Ischia*. Stabilimento Tipografico De Bonis.



- Rittman, A., & Gottini, V. (1980). L'isola d'Ischia. *Geologia Bollettino Servizio Geologico Italiano*, 101, 131–274.
- Rittmann, A. (1930). Geologie der Insel Ischia. *Zeitschrift für Vulkanologie Z. Vulkanol*, 6, 1–265.
- Ruffolo, F. (1923). *Progetto per provvedere di acqua potabile tutti i comuni dell'Isola d'Ischia. Relazione*. Stabilimento Tipografico Lubrano.
- Santi, B. (1955). Manifestazioni esalativo-idrotermali dell'Isola d'Ischia. *Bulletin Volcanologique S. II*, 16(1), 181–223. <https://doi.org/10.1007/BF02595981>
- Sbrana, A., Fulignati, P., Marianelli, P., Boyce, A. J., & Cecchetti, A. (2009). Exhumation of an active magmatic–hydrothermal system in a resurgent caldera environment: The example of Ischia (Italy). *Journal of the Geological Society*, 166(6), 1061–1073. <https://doi.org/10.1144/0016-76492009-030>
- Sbrana, A., Marianelli, P., & Pasquini, G. (2018). Volcanology of Ischia (Italy). *Journal of Maps*, 14(2), 494–503. <https://doi.org/10.1080/17445647.2018.1498811>
- Sbrana, A., & Toccaceli, R. M. (2011). Carta Geologica della regione Campania in scala 1:10.000 – Foglio 464, Isola di Ischia. Note illustrative. Regione Campania, Assessorato Difesa del Suolo. Litografia artistica cartografica, Firenze.
- Selva, J., Acocella, V., Bisson, M., Caliro, S., Costa, A., Della Seta, M., De Martino, P., de Vita, S., Federico, C., Giordano, G., Martino, S., & Cardaci, C. (2019). Multiple natural hazards at volcanic islands: A review for the Ischia volcano (Italy). *Journal of Applied Volcanology*, 8(5). <https://doi.org/10.1186/s13617-019-0086-4>
- Sepe, V., Atzori, S., & Ventura, G. (2007). Subsidence due to crack closure and depressurization of hydrothermal systems: a case study from Mt Epomeo (Ischia Island, Italy). *Terra Nova*, 19(2), 127–132. <https://doi.org/10.1111/j.1365-3121.2006.00727.x>
- Shahin, M. (2003). Hydrology and Water Resources of African Islands. In *Hydrology and Water Resources of Africa*. *Water Science and Technology Library* (Vol. 41, pp. 565–582). Springer. [https://doi.org/10.1007/0-306-48065-4\\_13](https://doi.org/10.1007/0-306-48065-4_13)
- Soulios, G. (2010). Springs (classification, function, capturing). *Bulletin of the Geological Society of Greece*, 43(1), 196. <https://doi.org/10.12681/bgsg.11174>
- Struckmeier, W. F., & Margat, J. (1995). *Hydrogeological maps: a guide and a standard legend* (Vol. 17). Heise.
- Tibaldi, A., & Vezzoli, L. (2004). A new type of volcano flank failure: The resurgent caldera sector collapse, Ischia, Italy. *Geophysical Research Letters*, 31(14), L14605. <https://doi.org/10.1029/2004GL020419>
- Trasatti, E., Acocella, V., Di Vito, M. A., Del Gaudio, C., Weber, G., Aquino, I., Caliro, S., Chiodini, G., de Vita, S., Ricco, C., & Caricchi, L. (2019). Magma degassing as a source of long-term seismicity at volcanoes: The Ischia Island (Italy) case. *Geophysical Research Letters*, 46(24), 14421–14429. <https://doi.org/10.1029/2019GL085371>
- Vezzoli, L. (1988). Island of Ischia. In L. Vezzoli (Ed.), *CNR Quaderni de "La ricerca scientifica"*, 114, 10 (p. 122). Consiglio Nazionale delle Ricerche.
- Vezzoli, L., Principe, C., Malfatti, J., Arrighi, S., Tanguy, J. C., & Le Goff, M. (2009). Modes and times of caldera resurgence: The b10 ka evolution of Ischia Caldera, Italy, from high-precision archaeomagnetic dating. *Journal of Volcanology and Geothermal Research*, 186(3-4), 305–319. <https://doi.org/10.1016/j.jvolgeores.2009.07.008>
- Vittecoq, B., Reninger, P. A., Violette, S., Martelet, G., Dewandel, B., & Audru, J. C. (2015). Heterogeneity of hydrodynamic properties and groundwater circulation of a coastal andesitic volcanic aquifer controlled by tectonic induced faults and rock fracturing – Martinique island (Lesser Antilles – FWI). *Journal of Hydrology*, 529, 1041–1059. <http://doi.org/10.1016/j.jhydrol.2015.09.022>